Journal of Sound and Vibration (1998) **218**(4), 587–598
Article No. sv981858

VIBRATION POWER FLOW IN A FLUID-FILLED CYLINDRICAL SHELL

M. B. Xu and X. M. Zhang

Department of Naval Architecture and Ocean Engineering,
Huazhong University of Science and Technology, 430074 *Wuhan*, *Hubei*,
P.R. China

(*Received* 19 *September* 1996, *and in final form* 24 *June* 1998)

The vibrational power flow from a line circumferential cosine harmonic force into an infinite elastic circular cylindrical shell filled with fluid is studied. To analyze the response of the shell, an integrated numerical method along the pure imaginary axis of the complex wavenumber domain is used. The results are discussed for a steel shell filled with fluid and vibrating in the $n = 0$, 1 and 2 circumferential modes. In order to evaluate the effect of the fluid, the results of a shell filled with fluid are compared with those of a shell *in vacuo*.

1. INTRODUCTION

Cylindrical shells filled with fluid are the practical elements of many types of engineering structure such as marine craft and airplanes. Machinery-induced vibration often occurs in these structures. In this paper, the action of the machine on a structure is modelled as a force and the main structure is considered as an infinite elastic circular cylindrical shell filled with fluid.

The concept of vibrational power flow analysis has been introduced in vibration and noise control. Goyder and White [1] investigated the near and far field power flow of infinite beans, plates and beam-stiffened plates with force and torque excition. Pavic [2] obtained expressions for energy flow in a cylindrical shell. These expressions were divided into three parts, two corresponding to extensional and flexural components similar to the expressions for flat plates, with the third concerning coupling effects which are introduced by curvature of the shell. Williams [3] arranged the energy flow components into five terms and derived the relationship between the energy flow in a shell and the normal acoustic intensity. Zhang and Zhang [4, 5] studied the input and transmitted power flow of an infinite cylindrical shell under the excitation of a line circumferential cosine force. Zhang and White [6] studied the input power of a shell due to point force excitation.

0022–460X/98/490587 + 12 $30.00/0

Experimental measurements of driving point accelerance and transfer accelerances have also been compared with theoretical predictions and good agreement was found in a frequency averaged sense.

In this paper, the vibrational power flow in a fluid-filled elastic shell is studied. Perhaps due to the complexity involved in solving and interpreting the dispersion equation, the forced excitation of this coupled system has received scant attention. Merkulov *et al*. [7] have briefly studied the point-force excitation of an infinte thin walled cylindrical shell filled with fluid, but their results are solely concerned with the relative transfer mobility of waves with varying branch and circumferential mode number; near field effects at the source necessary for the calculation of the input mobility were not included. Work by Fuller and Fahy [8] has been concerned with the solution and physical interpretation of the dispersion equation for a cylindrical shell filled with fluid. Fuller and Fahy also calculated the vibrational power distribution between the shell wall and fluid for free modes of propagation. The propagation of vibrational waves through wall joint in a fluid-filled shell has been studied by Xu *et al*. [9]. The results were also compared with those of a shell with wall joint *in vacuo*, and the presence of the fluid was found to increase the effects of wall joint on the wave propagation in lower frequency.

Fuller [10] calculated the input mobility of an infinite cylindrical shell filled with fluid. The spectral equations of motion of the shell–fluid system were employed in the analysis and results were presented for three circumferential orders of vibrational modes given by $n = 0$, 1 and 2. In the paper, the spatial Fourier transforms were used. In order to obtain the integral of the inverse transform, the author determined poles in the complex wavenumber domain and used the theorem of residues. The dispersion curves of this shell–fluid system are necessary to calculate the residues. Because of the complexity of the solution and physical interpretation of the dispersion equation for this coupled system, this method is difficult and complex.

In this paper, a simple method is used. The spatial Fourier transforms and the inverse transforms are used as in [10]. However, in order to avoid the solution of the dispersion equation, the theorem of residues is not used to obtain the integral. Instead, the result is obtained by integrating numerically along the imaginary axis of the complex wavenumber domain. A value of damping is assigned to the shell material in order to avoid singularities in the integrand function along the integration path. Using this method, Fuller [11] investigated the radiation of sound from an infinite elastic cylindrical shell excited by an internal monopole source. Xu *et al*. [12] also studied the input power flow of a cylindrical shell *in vacuo* due to a line force excitation by the same method. In order to verify this method, two other methods of calculation have also been used. The results show this method is accurate and simple.

2. FREE WAVE PROPAGATION OF THIS COUPLED SYSTEM

As the first step in the study of the forced response of the shell–fluid system, it is necessary to consider the free vibration behavior of the coupled system. The

cylindrical co-ordinate system employed and the modal shapes are shown in Figure 1. The vibrational motion of the shell is described by the Flügge shell equations as given in reference [9]. The normal mode shapes assumed for the displacement of the shell wall, associated with an axial wavenumber k_{ns}, are given by:

$$u = \sum_{s=1}^{\infty} \sum_{n=0}^{\infty} U_{ns} \cos(n\theta) \exp(\mathrm{i}\omega t + k_{ns}x)$$

$$v = \sum_{s=1}^{\infty} \sum_{n=0}^{\infty} V_{ns} \sin(n\theta) \exp(\mathrm{i}\omega t + k_{ns}x)$$

$$w = \sum_{s=1}^{\infty} \sum_{n=0}^{\infty} W_{ns} \cos(n\theta) \exp(\mathrm{i}\omega t + k_{ns}x) \tag{1}$$

The associated form of the pressure field in the contained fluid, which satisfies the acoustic wave equation, is expressed as

$$p = \sum_{s=1}^{\infty} \sum_{n=0}^{\infty} P_{ns} \cos(n\theta) J_n(k_s^r r) \exp(\mathrm{i}\omega t + k_{ns}x) \tag{2}$$

In equations (1) and (2), n is the circumferential modal number; subscript s denotes a particular branch of the dispersion curves; k_{ns} and k_s^r are the axial and radial wavenumbers, respectively, related to the free wavenumber k_0 by $(k_s^r)^2 = k_0^2 - k_{ns}^2$. Substitution of these forms into the Flügge shell equations results in the equations of motion in the terms of amplitudes of the three displacements and the acoustic pressure.

Application of the fluid momentum equation at the shell wall, $r = R$, produces

$$P_{ns} = [\omega^2 \rho_f / k_s^r J_n'(k_s^r R)] W_{ns} \tag{3}$$

where ρ_f is the density of the contained fluid, R is the mean radius of the shell, and the prime denotes differentiation with respect to the argument $k_s^r R$.

Substitution of equations (1, 2) and (3) into the shell equations results in the equations of motion of the coupled system, represented in symmetric matrix form,

$$[L_{3\times 3}][U_{ns} \quad V_{ns} \quad W_{ns}]^{\mathrm{T}} = [0 \quad 0 \quad 0]^{\mathrm{T}} \tag{4}$$

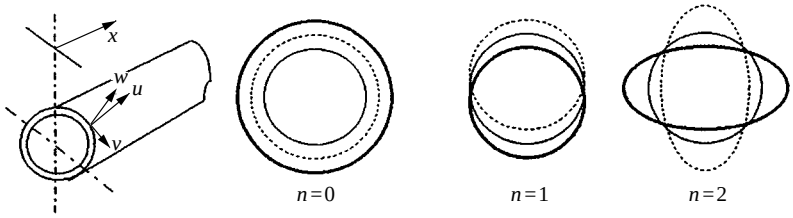

Figure 1. Co-ordinate system and modal shapes.

$$\begin{bmatrix} \lambda^2 + a' & b'\lambda & c'\lambda^3 + d'\lambda \\ b'\lambda & e'\lambda^2 + f' & g'\lambda^2 + h' \\ c'\lambda^3 + d'\lambda & g'\lambda^2 + h' & j' + k'\lambda^2 + l'\lambda^4 - FL \end{bmatrix} \begin{bmatrix} U_{ns} \\ V_{ns} \\ W_{ns} \end{bmatrix} = \begin{bmatrix} 0 \\ 0 \\ 0 \end{bmatrix} \tag{5}$$

$$\lambda = k_{ns}R, \quad a' = -(1-v)(1+K)n^2/2 + \Omega^2, \quad b' = (1+v)n/2, \quad c' = -K,$$
$$d' = v - K(1-v)n^2/2, \quad e' = -(1-v)(1+3K)/2, \quad f' = n^2 - \Omega^2,$$
$$g' = -(3-v)Kn/2, \quad h' = n, \quad j' = 1 + K(n^2-1)^2 - \Omega^2, \quad k' = -2n^2K,$$
$$l' = K, \quad \Omega^2 = \rho R^2\omega^2(1-v^2)/E, \quad K = h^2/12R^2 \tag{6}$$

where Ω is the non-dimensional frequency, v is the Possion's ratio of the shell material, h is the thickness of the shell wall, FL is the fluid loading term due to the presence of the fluid acoustic field.

The equations governing the motion of this coupled system are different from the *in vacuo* shell equations [12] by the presence of the fluid loading term, which is given by

$$FL = \Omega^2(\rho_f/\rho_s)(h/R)^{-1}(k_s^r R)^{-1}[J_n(k_s^r R)/J_n'(k_s^r R)] \tag{7}$$

where ρ_s is the density of the shell material. The non-dimensional radial wavenumber $k_s^r R$ can be written in terms of the shell non-dimensional frequency and axial wavenumber as

$$(k_s^r R)^2 = \Omega^2(C_L/C_f)^2 - (k_{ns}R)^2. \tag{8}$$

Expansion of the determinant of the amplitude coefficient in equation (5) provides the system characteristic equation. Due to the "non-linearity" of the equation, numerical methods have to be employed to find the desired eigenvalues. The eigenvalues will be either purely real, purely imaginary or complex, as for a shell vibrating *in vacuo*. For each circumferential modal number n, the wavenumber λ can be separated into two groups. The first group contains backward waves associated with a semi-infinite shell, $-\infty < x < 0$ (left side), excited at the edge at $x = 0$. The second group describes forward waves associated with a semi-infinite shell, $0 < x < \infty$ (right side), excited at the edge at $x = 0$. If λ is real or imaginary, one obtains a near field wave or a propagating wave respectively. If λ are complex in conjugate pairs, one obtains a pair of attenuated standing waves, which means that the wave amplitudes decay in one direction but the waves propagate in both directions.

3. INPUT POWER FLOW

To analyze the response of the system to a line force, applied around the circumference at $x = 0$, and specified by

$$p_0(\theta, t) = F_0 \cos(n\theta)\delta(0) \exp(i\omega t) \tag{9}$$

The shell displacements and applied forces as Fourier transforms are expressed as

$$u = 1/2\pi \int_{-\infty}^{\infty} \sum_{s=1}^{\infty} \sum_{n=0}^{\infty} U_{ns} \cos(n\theta) \exp(\mathrm{i}\omega t + k_{ns}x)\, \mathrm{d}k_{ns}$$

$$v = 1/2\pi \int_{-\infty}^{\infty} \sum_{s=1}^{\infty} \sum_{n=0}^{\infty} V_{ns} \sin(n\theta) \exp(\mathrm{i}\omega t + k_{ns}x)\, \mathrm{d}k_{ns}$$

$$w = 1/2\pi \int_{-\infty}^{\infty} \sum_{s=1}^{\infty} \sum_{n=0}^{\infty} W_{ns} \cos(n\theta) \exp(\mathrm{i}\omega t + k_{ns}x)\, \mathrm{d}k_{ns}$$

$$p_0 = 1/2\pi F_0 \cos(n\theta) \exp(\mathrm{i}\omega t). \tag{10}$$

Substituting equations (10) into the original equations of motion of the fluid-filled shell [9] gives the spectral equations of motion of the forced response of this coupled system,

$$\begin{bmatrix} \lambda^2 + a' & b'\lambda & c'\lambda^3 + d'\lambda \\ b'\lambda & e'\lambda^2 + f' & g'\lambda^2 + h' \\ c'\lambda^3 + d'\lambda & g'\lambda^2 + h' & j' + k'\lambda^2 + l'\lambda^4 - FL \end{bmatrix} \begin{bmatrix} \bar{U}_{ns} \\ \bar{V}_{ns} \\ \bar{W}_{ns} \end{bmatrix} = \begin{bmatrix} 0 \\ 0 \\ \Omega^2 F_0/(2\pi\rho_s h\omega^2) \end{bmatrix}. \tag{11}$$

The solutions of this equations are

$$\begin{bmatrix} \bar{U}_{ns} \\ \bar{V}_{ns} \\ \bar{W}_{ns} \end{bmatrix} = \begin{bmatrix} I_{11} & I_{12} & I_{13} \\ I_{21} & I_{22} & I_{23} \\ I_{31} & I_{32} & I_{33} \end{bmatrix} \begin{bmatrix} 0 \\ 0 \\ \Omega^2 F_0/(2\pi\rho_s h\omega^2) \end{bmatrix}. \tag{12}$$

where matrix $I_{3\times 3}$ is the inverse of matrix $L_{3\times 3}$. Thus the spectral radial displacement amplitude is

$$\bar{W}_{ns} = [\Omega^2 F_0/(2\pi\rho_s h\omega^2)] I_{33}. \tag{13}$$

Application of the inverse transform gives the radial displacement as

$$w(x/R, n, s) = \frac{\Omega^2 F_0}{2\pi\rho_s h\omega^2} \int_{-\infty}^{\infty} I_{33} \exp(k_{ns}x)\, \mathrm{d}(k_{ns}R). \tag{14}$$

The radial displacement at $x = 0$ is

$$w_{x=0} = \frac{\Omega^2 F_o}{2\pi\rho_s h\omega^2} \int_{-\infty}^{\infty} I_{33}\, \mathrm{d}(k_{ns}R). \tag{15}$$

The input power from the driving force is

$$P_i = \int_0^{2\pi} \tfrac{1}{2} \operatorname{Re}\{\mathrm{i}\omega F_0 w_{x=0}^*\} \cos^2(n\theta)\, \mathrm{d}\theta = \frac{\eta_n \pi}{2} \operatorname{Re}\{\mathrm{i}\omega F_0 w_{x=0}^*\} \tag{16}$$

where the * denotes the complex conjugate, and

$$\eta_n = \begin{cases} 2 & n = 0 \\ 1 & n \neq 0 \end{cases}.$$

The non-dimension input power is defined as

$$P_i' = \frac{P_i E}{F_0^2 \pi} \frac{\Omega}{\omega}. \tag{17}$$

From the theory of matrix, I_{33} can be written in terms of the elements of matrix $L_{3\times 3}$ as

$$I_{33} = (L_{11}L_{22} - L_{12}L_{21})/(\det|L|). \tag{18}$$

The integral in equation (15) must be evaluated. One way is to determine poles in the complex wavenumber domain and use the theorem of residues, just as in reference [10]. Because the solution of the dispersion equations for this coupled shell–fluid system is necessary, and because of the complexity involved in solving the dispersion equations, this method is complex.

In this paper, a simple method discussed in reference [12] is used to calculate the integral in equation (15). This method is to integrate numerically along the pure imaginary axis of the complex wavenumber domain. Some damping is introduced into the shell material in order to avoid singularities in the integrand function along the integration path. Damping is introduced into the shell material by modifying Young's modules E to make it more complex such that $E' = E(1 - \mathrm{i}\eta)$.

In order to obtain the integral, the upper truncation point of the integral range has to be decided. In this paper, the value of integral in $[-b, b]$ is compared with that in $[-0{\cdot}5b, 0{\cdot}5b]$. If the difference is less than 1%, then b will be taken as the upper truncation point. When the integral range is decided, it is divided into many small integral ranges and the Gauss integral method is used in each integral range. This method is found to provide sufficient accuracy and the value of loss factor η has an insignificant effect on the final results.

4. RESULTS AND DISCUSSIONS

The input power is evaluated for a steel shell filled with fluid and vibrating in the $n = 0$, 1 and 2 circumferential modes. For comparison, the input power of an identical shell vibrating *in vacuo* was studied by using two other methods (see [12]).

In order to investigate the relationship between the input power flow and the propagating waves, the dispersion curves of this shell–fluid system are given first.

Figure 2 shows typical dispersion curves for wave propagating with a circumferential modal order of $n = 0$ in a shell filled with water. For the sake of brevity, only the propagating waves (the wavenumber λ is purely imaginary) are plotted here.

It can be seen from Figure 2 that two propagating waves exist at low frequencies (torsional motion is uncoupled and thus not plotted). The first branch, $s = 1$, is

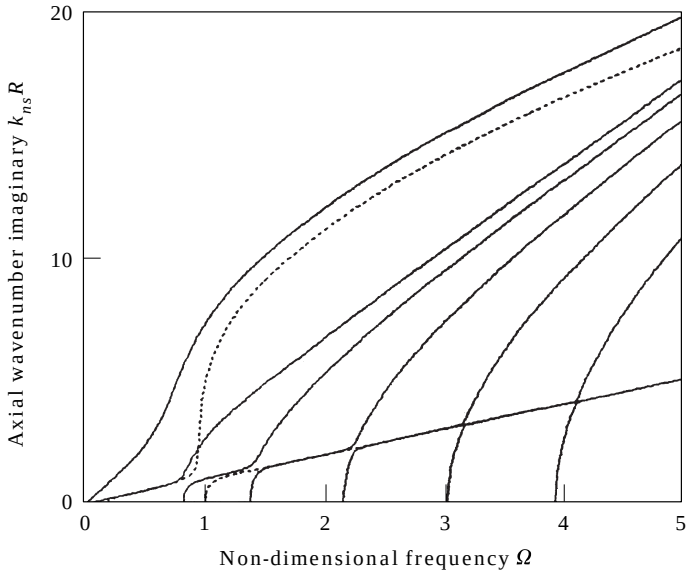

Figure 2. Dispersion curves for a steel shell (only propagating waves are plotted). $\rho_s = 7800$ kg/m^3; $E = 1{\cdot}92 \times 10^{11}$ N/m^2: $v = 0{\cdot}3$; $h/R = 0{\cdot}05$; ——, water-filled shell; -----, *in vacuo* shell; $n = 0$.

close to that representing a fluid wave in a rigid walled tube. The second branch, $s = 2$, is close to that representing the *in vacuo* shell wave at low frequencies and is thus largely uncoupled from the fluid. A third branch, $s = 3$, intercept at $\Omega = 0{\cdot}83$. Initially this branch follows closely that of the corresponding extensional *in vacuo* shell wave until at $\Omega = 1{\cdot}373$ when it turns sharply to approach the second rigid walled acoustic mode. Near this frequency a fourth branch, $s = 4$, cuts on as a fluid wave in a tube with compliant walls and then turns into a plateau (the wavenumber λ arises linearly versus frequency Ω) to change its behavior to that of an extensional *in vacuo* shell wave largely uncoupled from the fluid. Similarly all highly branches cut on as fluid waves and then quickly change their behavior to that of an extensional *in vacuo* shell waves while the previous construct shell-type branch converts to a fluid waves. All the plateau parts of these propagating waves form a straight line and this line closely follows that of the corresponding extensional *in vacuo* shell wave. The cut-on frequencies of these propagating waves are $\Omega = 2{\cdot}15$, $3{\cdot}02$ and $3{\cdot}902$.

Dispersion curves for the $n = 1$ and higher circumferential modal numbers exhibit behavior similar to that of $n = 0$ apart from a few major differences. At low frequencies for the $n = 1$, there exists only one propagating wave which corresponds to beam type motion of the shell. And there are two series of plateau arising from coincidence of torsional and extensional shell waves with duct type fluid waves. All the two series of plateau parts from two straight lines following closely those of the corresponding torsional and extensional *in vacuo* shell waves. Waves with higher circumferential modal numbers ($n > 1$) have dispersion characteristics similar to those of the beam mode except that the wave has a non-zero cut on frequency and the points of coincidence are shifted to higher

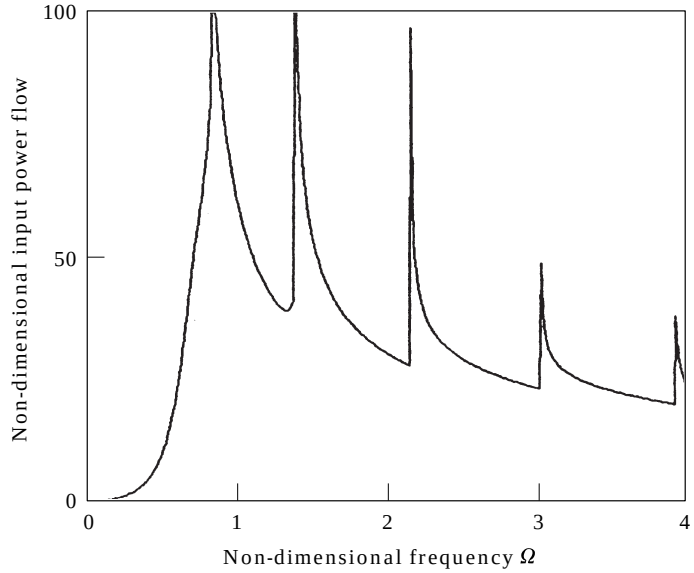

Figure 3. The input power into a steel shell by using the method of residues. $n = 0$.

frequencies. Dispersion curves for these higher circumferential modes are not plotted for brevity.

In order to verify the method used in this papaer, the input power flow into a shell for the $n = 0$ circumferential modal number is calculated by using the method of residues. Figure 3 shows the non-dimension power flow plotted against non-dimension frequency Ω.

The results obtained by using the method described in this paper are plotted in Figures 4, 5 and 6. From Figure 4, we can conclude that the results obtained by

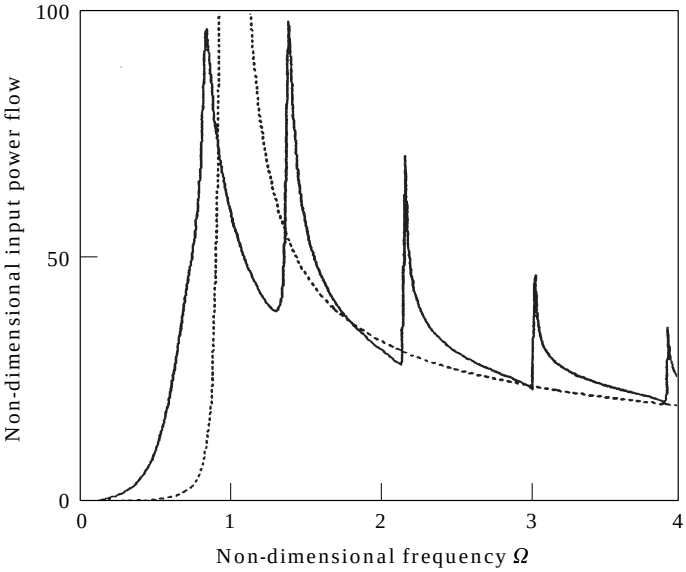

Figure 4. The input power into a shell. $n = 0$, $\eta = 0{\cdot}1$. ——; water-filled; -----, *in vacuo*.

using the numerical intergrate method show good agreement to those obtained by using the method of residues.

The input power for the $n = 0$ circumferential mode shape is given in Figure 4. The input power of the *in vacuo* shell has two peaks at $\Omega = 1{\cdot}0$ and 1·0125. These are the cut-on frequency and the ring frequency, respectively. The input power of the fluid-filled shell has peaks at $\Omega = 0{\cdot}83$, 1·38, 3·02 and 3·9. These correspond to cut-on frequencies of higher propagation branches in Figure 2. At very low frequencies the input power of the fluid-filled shell is very low and close to the *in vacuo* result. With the increase in frequency ($\Omega < 0{\cdot}9$), the input power is still small but larger than that of the *in vacuo* shell. At higher frequencies ($\Omega = 1{\cdot}0$), when the input power of the *in vacuo* shell rises dramatically to its peaks, it will be larger than the result of the fluid-filled shell. When the frequency increases further, it will be smaller than the result of the fluid-filled shell again. It can be seen that the contained fluid has the effect of reducing the magnitude of the resonant response and spreading the resonance over a wider frequency range than *in vacuo*. At higher frequencies ($\Omega > 1{\cdot}0$), the input power of the fluid-filled shell is close to the *in vacuo* result apart from peaks which correspond to the cut on frequencies of higher propagation branches. At frequencies near these peaks, the input power is much larger than the *in vacuo* result.

The input power flow for the $n = 1$ mode of vibration is plotted in Figure 5. The input power of the shell *in vacuo* has two peaks at $\Omega = 1{\cdot}0$ and 1·425. The input power of the fluid-filled shell has peaks at $\Omega = 1{\cdot}3$, 1·8, 2·9 and 3·5. These frequencies correspond to the cut-on frequencies of higher propagation branches. At low frequencies, the input power of the fluid-filled shell is less than the *in vacuo* results. As there exists only one propagating

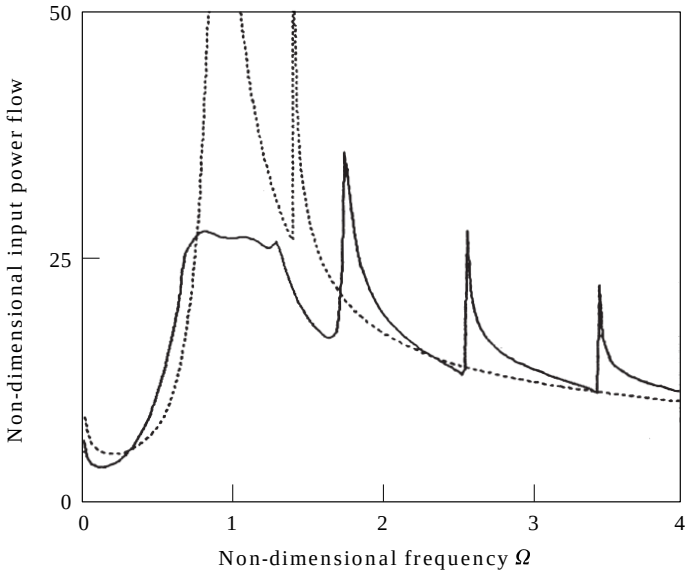

Figure 5. The input power into a shell. $n = 1$, $\eta = 0{\cdot}1$. ——; water-filled; -----, *in vacuo*.

branch, $s = 1$, this branch corresponds to beam-like motion of the shell. The major effect of the contained fluid is an increase in the mass of the system, which leads to a reduction in shell radial response for a given force. With the increase in frequency, near $\Omega > 0{\cdot}5$, as the first fluid wave ($s = 2$) cuts on, the input power increases markedly as the fluid and the shell become strongly coupled. The input power of the fluid-filled shell is larger than that in the *in vacuo* results. The contained fluid again has the effect of reducing the magnitude of the resonant response and spreading the resonance over a wider frequency range than *in vacuo*. In the frequency range $0{\cdot}8 < \Omega < 1{\cdot}8$, the input power of the fluid-filled shell is less than that in the *in vacuo* results which have two peaks in this range. At higher frequencies, $\Omega > 1{\cdot}8$, the input power is close to that in the *in vacuo* results apart from peaks which correspond to the higher propagation branches cutting on. At frequencies near these peaks, the input power is much larger than that in the *in vacuo* results as in the case $n = 0$ mode.

The input power flow for the $n = 2$ mode of vibration is plotted in Figure 6. The results for the $n > 1$ mode are similar to the $n = 1$ mode apart from a few major differences. Because at very low frequencies, there is no propagating wave (a non-dimension cut-on frequency exists), so the input power flow is zero. The cut-on frequency of the fluid-filled shell is less than that of the shell *in vacuo*. With the increase in circumferential modal number n, the cut-on frequency will increase, just as that *in vacuo*.

The characteristics of wave propagation in a fluid-filled shell are important and the cut-on frequencies of the propagating waves are also important and not easy to locate. With the method presented in this paper, we can obtain the input power easily. Further, because the input power of the fluid-filled shell has peaks at

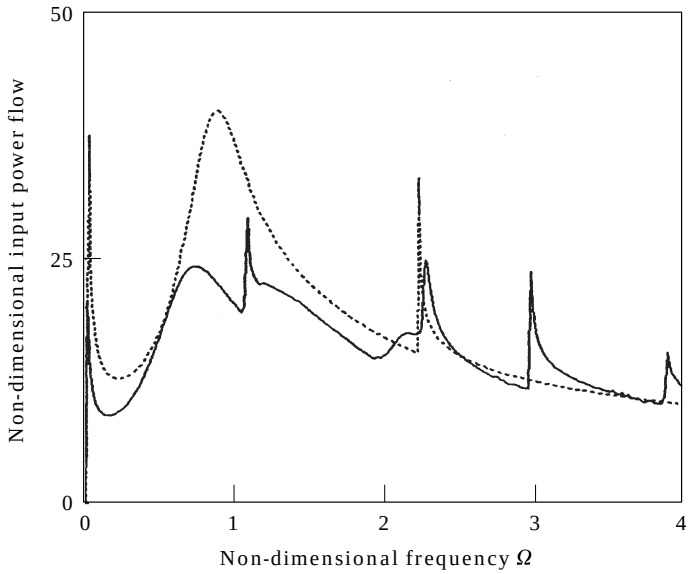

Figure 6. The input power into a shell. $n = 2$, $\eta = 0{\cdot}1$. ——; water-filled; -----, *in vacuo*.

frequencies corresponding to cut-on frequencies, we can easily obtain approximate cut-on frequencies of this coupled system.

5. CONCLUSIONS

The input power flow from a line circumferential cosine harmonic force into a fluid-filled shell is studied by numerical integration along the purely imaginary axis of the complex wavenumber domain. Results are obtained for a shell vibrating in various circumferential modes. For comparison, the input power of an identical shell vibrating *in vacuo* is also studied. The results are discussed and the system behavior is explained in terms of free wave propagation characteristics. The input power of the fluid-filled shell has peaks at frequencies corresponding to cut-on frequencies of propagation branches. Generally, when the frequencies are high and away from these peaks, the input power is close to the *in vacuo* result. At frequencies near these peaks, the input power is much larger than the *in vacuo* results. The results show this method is simple and accurate. Use of this method to calculate the response of other more complex systems is the subject of future work.

REFERENCES

1. H. G. D. Goyder and R. G. White 1980 *Journal of Acoustical Society of America* **68**, 59–96. Vibrational power flow from machines into built-up structures.
2. G. Pavic 1990 *Journal of Sound and Vibration* **142**, 293–310. Vibrational energy flow in elastic circular cylindrical shells.
3. E. Willams 1991 *Journal of Acoustical Society of America* **89**, 1615–1622. Structural intensity in thin cylindrical shells.
4. X. M. Zhang and W. H. Zhang 1990 *Proceedings of ASME PVP*. Vibrational power flow in a cylindrical shell.
5. W. H. Zhang and X. M. Zhang 1991 *Proceedings of ASME PVP*. Vibrational power flow in a cylindrical shell with periodic stiffeners.
6. X. M. Zhang and R. G. White 1993 *The 4th International Congress on Intensity Techniques, France*. Vibrational power input to a cylindrical shell due to point force excition.
7. V. N. Merkulov, V. YU. Prikhodko and V. V. Tyutekin 1979 *Soviet Physics-Acoustics* **25**, 51–54. Normal modes in a thin cylindrical elastic shell filled with fluid and driven by forces specified on its surface.
8. C. R. Fuller and F. J. Fahy 1982 *Journal of Sound and Vibration* **81**, 501–518. Characteristics of wave propagation and energy distributions in cylindrical elastic shells filled with fluid.
9. M. B. Xu, X. M. Zhang and W. H. Zhang 1995 *Proceedings, International Conference on Structural Dynamics, Vibration, Noise and Control, SDNVC*'95, *Hong Kong*. The effect of wall discontinuities on the wave propagation in a fluid-filled elastic cylindrical shell.
10. C. R. Fuller 1983 *Journal of Sound and Vibration* **87**, 409–427. The input mobility of an infinite circular cylindrical elastic shell filled with fluid.
11. C. R. Fuller 1986 *Journal of Sound and Vibration* **109**, 259–275. Radiation of sound from an infinite cylindrical elastic shell excited by an internal monopole source.
12. M. B. Xu and X. M. Zhang 1997 *Proceedings, 8th National Marine Vibration and Noise Conference, Wuhan, China*. The input vibrational power flow into a cylindrical shell calculated by three methods (in Chinese).

APPENDIX: LIST OF SYMBOLS

C_f = fluid acoustic free wave speed
C_L = shell extension phase speed
E = Young's modulus
FL = fluid loading term
h = shell wall thickness
$\mathrm{i} = \sqrt{-1}$
$J_n 0$ = Bessel function of order n
k_0 = free wavenumber
k_{ns} = axial wavenumber
k_s^r = radial wavenumber
n = circumferential modal number
P_i = input power flow
P_i' = non-dimension input power flow
R = shell mean radius
s = branch number
u, v, w = shell displacements
U_{ns}, V_{ns}, W_{ns} = shell displacement amplitudes
ρ_f = density of fluid
ρ_s = density of shell
v = Poisson's ratio
ω = circular frequency
Ω = non-dimension frequency
λ = non-dimension wavenumber
η = loss factor
$(^*)$ = complex conjugate
$\bar{(\ )}$ = Fourier transform